Structure of polymorphic phases in zinc arachidate LB multilayers

N. Prasanth Kumar[a,1], S.S. Major[a,*], Satish Vitta[b], S.S. Talwar[a], Ajay Gupta[c], B.A. Dasannacharya[c]

[a] *Department of Physics, Indian Institute of Technology Bombay, Mumbai 400076, India*
[b] *Department of Metallurgical Engineering and Materials Science, Indian Institute of Technology Bombay, Mumbai 400076, India*
[c] *Inter-University Consortium for DAE Facilities, Indore 452017, India*

Abstract

The 3D structure of zinc arachidate (ZnA) LB multilayers transferred at different subphase pH has been studied using X-ray scattering and FT-IR spectroscopy. The molecular packing in ZnA multilayers shows an unusually strong dependence on subphase pH, not observed earlier in LB multilayers of divalent fatty acid salts. In all four polymorphic phases, α, β, γ and δ with characteristic 3D structures were observed and in most cases, two or more phases were found to coexist. The δ-phase, which corresponds to the largest alkyl chain tilt angle of ∼32°, is stable over the complete range of subphase pH investigated and appears as a single phase at a subphase pH of ∼6.5. It corresponds to a rotator phase like 'loose packing' of molecules tilted at an angle of 32° with respect to chain axis, packed in a hexagonal layer cell. The subcell packing changes from hexagonal to orthorhombic and the angle of tilt decreases from 32° (δ-phase) to nearly 0° (α-phase) with increasing pH up to 7.4. The dominant phase at a pH of ∼7.4 (α-phase) has a close packed herringbone structure. However at higher subphase pH, the 'rotator like' δ-phase regains prominence. The interface morphology of different polymorphic phases is found to be unique, independent of the subphase pH at which the monolayers are transferred.

Keywords: Langmuir–Blodgett; Multilayer; Zinc arachidate; Molecular packing; Polymorphs

1. Introduction

Organic multilayers deposited by the Langmuir–Blodgett (LB) technique have been the subject of intense research due to the rich variety of organized molecular layered structures they provide [1,2]. Long chain fatty acids and their divalent arachidate/stearate metal salts such as cadmium arachidate (CdA) have been the most extensively studied LB systems and their 3D structure and molecular packing have been investigated using a variety of techniques [3–10]. The molecular packing in the divalent metal fatty acid salt multilayers has been reported [5] to depend on the electronegativity of the metal ion and in most cases, corresponds to the closed packed structures proposed by Kitaigorodskii [11] for long chain organic compounds. These structures are based on orthorhombic, monoclinic and triclinic subcells in which the molecular chains are tilted at specific angles determined essentially by the constraints of optimizing chain packing density in the plane perpendicular to the chains. It has however been reported [12] that zinc arachidate (ZnA) multilayers do not follow this trend, and the molecules pack in a distorted hexagonal layer cell with chains tilted at an angle of ∼30° towards the nearest neighbour. In a subsequent study, it has been shown by powder XRD studies, that ZnA multilayers transferred at different subphase pH consist of different types of layered structures characterized by different bilayer periods and hence different chain tilt angles [13]. These observations suggest that even in divalent fatty acid salt systems, the molecular packing arrangement in the transferred multilayers and its dependence on subphase conditions is not completely understood.

In the present work, the 3D structure of the polymorphic phases in ZnA multilayers transferred at nominal subphase

pH values ranging from 6.5 to 8.0 has been studied using X-ray scattering and FT-IR spectroscopy techniques. Below a subphase pH of 6.5, the multilayers consisted of a mixture of arachidic acid and zinc arachidate molecules [13]. Hence a pH range of 6.5–8.0 was chosen for the present investigations.

2. Experimental details

Zinc arachidate multilayers were made by the conventional LB deposition technique using a KSV 3000 LB instrument. Arachidic acid (Aldrich, 99%) with HPLC grade chloroform as solvent (1 mg/ml) was used to spread the monolayer on Millipore ultrafiltered water subphase (resistivity = 18.2 MΩ cm) containing $ZnCl_2$ (concentration, 10^{-5} M). The subphase pH was adjusted to desired values by adding dilute HCl, $NaHCO_3$ and NaOH solution to the subphase. The layers were transferred at a constant surface pressure of 30 mN/m and at a substrate dipping speed of 3 mm/min. A total of 25 monolayers were transferred on quartz and CaF_2 substrates for all the studies, with unit transfer ratio.

X-ray reflectivity measurements were carried out using a Siemens D5000 diffractometer with Cu Kα radiation. Three types of scanning geometries; the longitudinal θ–2θ specular scan, the longitudinal offset scan (at an offset angle of 0.3°) and transverse scan were used. A razor blade creates a slit of ∼0.02 mm at the sample and results in 0.02° divergence of the incident beam. The exit beam path consists of a soller slit, LiF(1 0 0) monochromator and a NaI scintillation detector.

Grazing incidence X-ray diffraction (GIXD) studies were performed using synchrotron radiation of wavelength 0.155 nm at the Italian synchrotron source, ELETTRA (SAXS beamline). An asymmetrically cut Si(1 1 1) double crystal both selects and monochromatizes the 0.155 nm radiation. A guard slit of size 2.0 mm × 0.05 mm ($H \times V$) defines the illuminated area on the sample surface. A 1D gas filled detector, with an angular resolution of 0.05° was used to detect the diffracted beam whose size was defined by a 1.6 mm × 0.6 mm exit slit. The angle of incidence was kept close to the critical angle for total reflection, ∼0.3° and the diffraction spectrum was studied in the range 10–60°.

FT-IR studies were carried out on multilayers transferred on CaF_2 substrates using a Nicolet (Impact 400) instrument.

3. Results

The reflectivity scans (specular and off-specular) from the ZnA multilayers transferred onto quartz substrates at different subphase pH are shown in Fig. 1. In most cases the multilayers exhibit two types of layered structures corresponding to different bilayer periods, except for the multilayer transferred at a pH of ∼6.5. The bilayer period, which is the average distance between two successive head groups, can be determined from the peak positions by using the Bragg equation modified for refraction effect [14]. The corresponding alkyl chain tilt angles were calculated using a value of 2.76 nm for the typical length of an arachidate molecule [2].

The specular reflectivity scan (Fig. 1(a)) for the ZnA multilayers transferred at a nominal subphase pH of 6.5 exhibits a single phase layered structure with a bilayer period of 4.7 nm (hereafter called δ-phase). Increasing the subphase pH to 6.8 results in the formation of a two phase layered structure with bilayer periods of 4.7 nm (δ-phase) and 5.0 nm (hereafter called γ-phase), as seen in Fig. 1(b). Similar reflectivity scans were observed for multilayers transferred in the subphase pH range of 6.8–7.2, except for small variations in relative intensities of Bragg peaks corresponding to the two phases. The reflectivity scan from multilayer transferred at a subphase pH of 7.3 (Fig. 1(c)) still shows the coexistence of two different layered structures but now with bilayer periods of ∼4.7 nm (δ-phase) and ∼5.3 nm (hereafter called β-phase). The ZnA multilayer transferred at a subphase pH of 7.4 however shows drastically different features. As shown in Fig. 1(d), the dominant phase in these multilayers has a period of 5.5 nm (hereafter called α-phase), together with very weak peaks corresponding to δ-phase. Multilayers transferred in the pH range

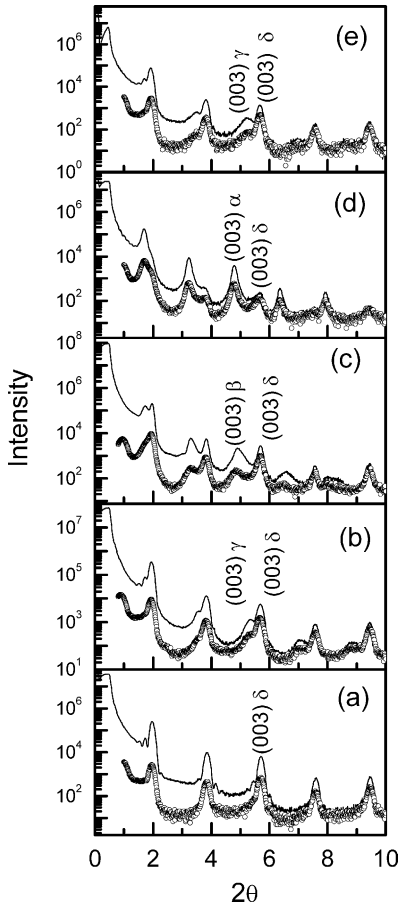

Fig. 1. Longitudinal specular (solid line) and off-specular (open circles) scans for the ZnA multilayers transferred at subphase pH values of (a) 6.5, (b) 6.8, (c) 7.3, (d) 7.4 and (e) 7.6, showing the different types of layered structures present in ZnA multilayers.

Table 1
GIXR and GIXD results of ZnA multilayers transferred at different subphase pH ('h' and 'r' refer to hexagonal and rectangular 2D lattices, respectively)

Subphase pH	Bilayer period (nm) from GIXR (tilt angle, °)		Intralayer *d*-values (nm) from GIXD, for prominent peaks and their indexing	Phase
6.5	4.7 (32)	–	0.45: (1 0) h 0.22: (2 0) h	δ
6.8	4.7 (32)	5.0 (26)	0.44: (1 1) r of R[±1, 0] or (1 0) h 0.39: (0 2) r of R[±1, 0] 0.24: (1 3) r of R[±1, 0] 0.22: (2 2) r of R[±1, 0]	δ + γ
7.3	4.7 (32)	5.3 (18)	–	δ + β
7.4	4.7 (32)	5.5 (∼5)	0.44: (1 0) h 0.40: (1 1) r of R[0, 0] 0.36: (0 2) r of R[0, 0] 0.24: (2 0) r of R[0, 0] 0.21: (1 3) r of R[0, 0] 0.20: (2 2) r of R[0, 0]	α + δ
7.6	4.7 (32)	5.0 (26)	0.44: (1 1) r of R[±1, 0] or (1 0) h 0.37: (2 0) r of R[±1, 0] 0.23: (1 3) r of R[±1, 0] 0.22: (2 2) r of R[±1, 0]	δ + γ

of 7.4–7.5 show identical reflectivity behaviour. Increase of subphase pH to 7.6 shows the re-emergence of δ-phase together with the γ-phase as seen in Fig. 1(e). All the multilayers transferred up to subphase pH of ∼8 exhibited similar phase mixture, as seen at a pH of 7.6. The above results are summarized in Table 1.

The longitudinal offset θ–2θ scan which probes the diffusely scattered intensity is also shown in Fig. 1, together with the specular reflectivity scans for all the multilayers. The diffusely scattered intensity exhibits peaks at the Bragg positions corresponding to all the polymorphic phases in all the cases. This clearly indicates that the interface morphological features are replicated along the vertical growth direction, independent of the type of polymorph present in the multilayer. The ratio of diffusely scattered intensity to the specular intensity is however different for the different polymorphs, indicating qualitatively that the nature of interfaces at different polymorphs is not identical.

In order to investigate the nature of interface morphology at the different polymorphic phases in multilayers transferred at different subphase pH values, transverse (ω) scans were performed at high-order Bragg peak positions. The transverse scans from the fourth-order Bragg peak positions corresponding to the δ-phase from ZnA multilayers transferred at all the subphase pH values discussed above, the γ-phase observed at subphase pH values of 6.8 and 7.6, the β- and α-phases observed at subphase pH values of 7.3 and 7.4, respectively, have been plotted and are shown in Fig. 2(a)–(d). The diffusely scattered intensity distribution for the δ-phase, which is present in all the multilayers and the α-phase, which is present in the multilayer transferred at a subphase pH of 7.4 are found to be nearly identical. Similarly, the γ-phase, which is present in two of the multilayers (subphase pH values of 6.8 and 7.6) and the β-phase, which is present for the multilayer transferred at subphase pH of 7.3 were identical. The interface morphology is defined by the roughness, roughness correlation in the plane of the interfaces and the nature of roughness correlation between the interfaces along the growth direction. The broad maxima observed for the δ- and α-phases are typ-

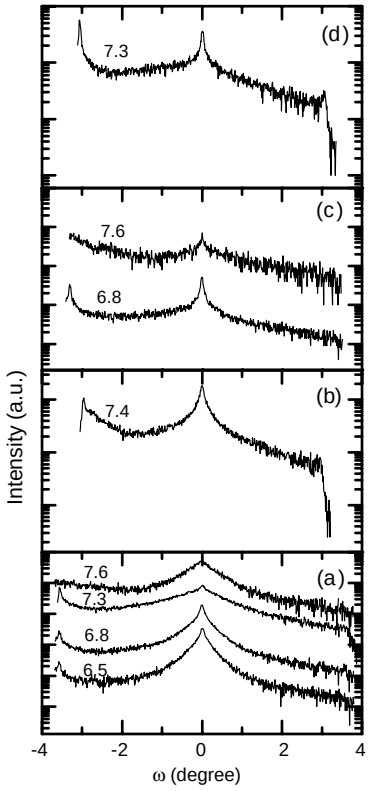

Fig. 2. Transverse scans at fourth-order Bragg peak position for the ZnA multilayers corresponding to (a) δ-phase, (b) α-phase, (c) γ-phase and (d) β-phase, showing the nature of interface morphologies at different phases.

ical of scattering behaviour observed in self-affine surfaces which have an in-plane correlation length greater than the coherence length of the incident X-ray beam [15]. The scattered intensity distribution from γ- and β-phases however exhibit a sharp transverse scan peak at the specular position in contrast to δ- and α-phases. Such peak shapes have been earlier observed in case of liquid-crystalline polymer LB multilayers and are modeled considering self-affine interfaces with a finite correlation length [16]. A more detailed analysis of these features is presently in progress. The results however show that the diffusely scattered intensity distributions are specific to the polymorphs, suggesting that each of these polymorphs have characteristic interface morphology, which does not depend on the subphase pH at which the polymorphic phases appear.

The intralayer molecular packing in ZnA multilayers transferred at different subphase pH values was studied using grazing incidence X-ray diffraction. The results are shown in Fig. 3 and the structural parameters obtained from these are also summarized in Table 1. The diffraction pattern of a ZnA multilayer transferred at a subphase pH of 6.5 (Fig. 3(a)) consists of a strong peak at 20.05° and a weak, broad peak at 41.55°. The ZnA multilayer transferred at a subphase pH of 6.8 exhibits broad peaks at 20.05° and 22.95° along with some weak over lapping peaks seen at ∼40°. A similar diffraction pattern was observed for the ZnA multilayer transferred at a subphase pH of 7.2. In contrast, the ZnA multilayer transferred at a subphase pH of 7.3 shows a featureless diffraction scan (Fig. 3(c)), indicating a disordered in-plane structure. Fig. 3(d) shows the diffraction pattern from multilayers transferred at a subphase pH of 7.4, which consists of three strong and resolvable peaks at 20.55°, 22.50° and 25.24° along with weak peaks at ∼38°, 43° and 46°. The diffraction pattern from the multilayers transferred at a subphase pH of 7.6 (Fig. 3(e)), however, is quite similar to that of the multilayer transferred at a subphase pH of 6.8 (Fig. 3(b)). The pattern exhibits a strong peak at 20.55° and weak peaks at 23.9°, 40.4° and 42.4°.

The molecular packing in ZnA multilayers has also been studied by FT-IR spectroscopy. The CH_2 scissoring mode of the alkyl chain is known to be sensitive to intermolecular interactions and has been used to understand molecular packing in *n*-alkanes, fatty acids and their salts in bulk crystal form [17] as well as in LB films [18,19]. It appears as a singlet (∼1465 cm^{-1}) when the molecular packing corresponds to one molecule per unit cell, based on oblique or hexagonal 2D sublattices in the plane perpendicular to the chains. The scissoring band however splits due to crystal field effect to form a doublet (1462 and 1472 cm^{-1}) for orthorhombic subcell packing having two molecules per unit cell in herringbone arrangement, which is based on a rectangular 2D sublattice in the plane perpendicular to the chains. The scissoring vibration band has been monitored for ZnA multilayers transferred on CaF_2 substrates at different subphase pH values and the results are shown in Fig. 4. It may be mentioned here that for all the multilayers transferred in the subphase pH range of 6.5–8.0, FT-IR spectra exhibited absorption bands at ∼1540 cm^{-1} corresponding to asymmetric (COO^-) stretching vibrations of the carboxylate group and no peak at ∼1700 cm^{-1} due to carbonyl stretching of the carboxylic acid group was observed, indicating that the multilayers were in pure arachidate (salt) form and not a mixture of arachidic acid and arachidate salt. Fig. 4(a) and (b) show that for the ZnA multilayers transferred at subphase pH values of 6.5 and 6.8, the CH_2 scissoring vibration exhibits a single band at 1465 cm^{-1}. However, for the multilayer transferred at a subphase pH of 7.3, the CH_2 scissoring vibration (Fig. 4(c)) shows a peak at 1470 cm^{-1} with a shoulder at 1459 cm^{-1}. As the subphase pH is increased to 7.4, the

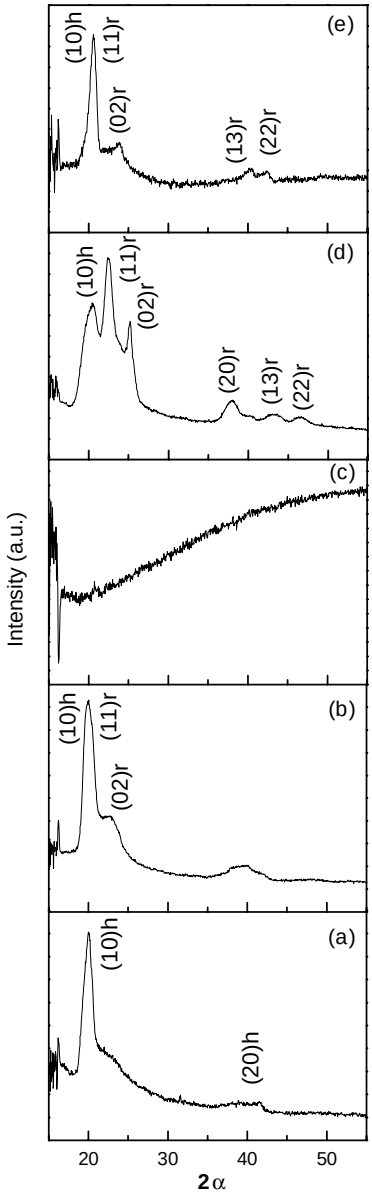

Fig. 3. GIXD patterns of ZnA multilayers transferred at subphase pH values of (a) 6.5, (b) 6.8, (c) 7.3, (d) 7.4 and (e) 7.6, showing the intralayer structure of ZnA multilayers.

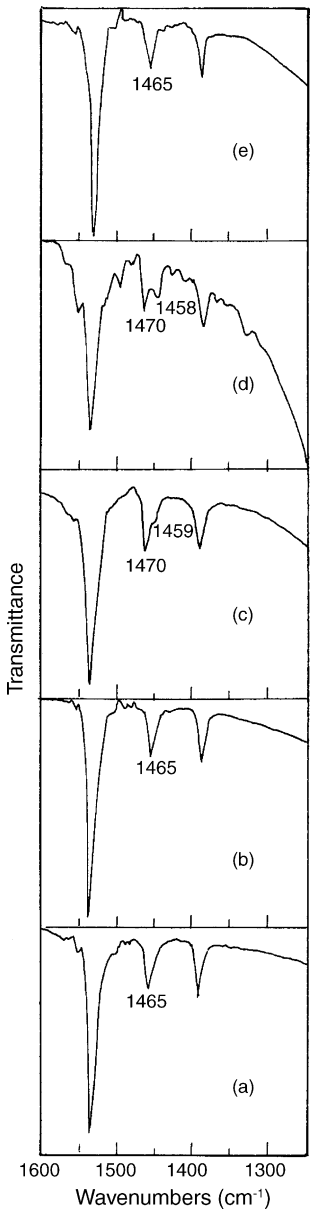

Fig. 4. FT-IR spectra of ZnA multilayers showing the CH_2 scissoring vibration of ZnA multilayers transferred at subphase pH values of (a) 6.5, (b) 6.8, (c) 7.3, (d) 7.4 and (e) 7.6, showing the nature of molecular packing in ZnA multilayers.

CH_2 scissoring vibration clearly splits to form a doublet at ∼1470 and ∼1458 cm^{-1} (Fig. 4(d)). However, for a higher subphase pH value of 7.6, the CH_2 scissoring vibration again appears as a singlet at ∼1465 cm^{-1} in Fig. 4(e).

4. Discussion

The understanding of molecular packing in LB multilayers has generally been on the lines of the work of Kitaigorodskii [11] on solid state structures of long chain organic compounds. The orthorhombic subcell packing proposed by Kitaigorodskii is among the frequently observed packing arrangements in LB multilayers which is also referred to as herringbone packing in which the orientation of the zig-zag or long axis of adjacent rows of molecules alternates to facilitate close packing of alkyl chains. Table 2 summarizes the parameters for some of the close packed arrangements based on orthorhombic subcell packing. The ideal close packed structure R[0, 0] corresponds to a stacking of chains perpendicular to the layer plane, while there are two other close packed arrangements with molecular chains tilted by specific angles towards specific directions.

The reflectivity scan shown in Fig. 1(a) for the ZnA multilayer transferred at a subphase pH of 6.5 consists of a layered structure characterized by a bilayer period of 4.7 nm, which corresponds to a chain tilt angle of ∼32° (δ-phase). The corresponding GIXD pattern in Fig. 3(a) shows a strong low-order peak. The existence of a single low-order GIXD peak as well as the appearance of the CH_2 scissoring band as a singlet indicates that the intralayer molecular packing in the ZnA multilayer is based on a hexagonal layer cell. The GIXD peaks can thus be indexed as (1 0) and (2 0) reflections of a hexagonal lattice with a lattice constant of 0.51 nm, which corresponds to an unusually large mean molecular area of 0.23 nm^2. As discussed in an earlier report [20], this type of molecular packing has not been observed in LB multilayers of divalent fatty acid salts but such loosely packed structures called 'rotator phases' are known to exist in long chain alkanes at higher temperatures [21].

For the ZnA multilayer transferred at a subphase pH of 6.8, the reflectivity scan shows the dominance of Bragg peaks corresponding to the δ-phase along with weak Bragg peaks corresponding to γ-phase which is characterized by a chain tilt angle of ∼26°. The GIXR and GIXD results of Fig. 2(b), summarized in Table 1, when compared with the data in Table 2 show that the two low-order peaks at 20.05° and 22.95° can be indexed as the (1 1) and (0 2) reflections of the R[±1, 0] type layer packing, respectively, which is characterized by a tilt angle of 27° towards the nearest neighbour direction. It may be noted that the (1 1) reflection of the 2D rectangular lattice (γ-phase) in this case almost overlaps with the (1 0) reflection of the 2D hexagonal lattice (δ-phase), which dominates the

Table 2
Calculated *d*-values (using λ = 0.155 nm) for allowed in-plane reflections from 2D layer cells, based on Kitaigorodskii's [11] orthorhombic (R) subcell packing

Layer packing type	Layer cell (nm)	Tilt angle (°)	*d* (nm)				
			(1 1)	(0 2)	(2 0)	(1 3)	(2 2)
R[0, 0]	$a = 0.496$; $b = 0.742$; $\gamma = 90°$	0	0.412	0.371	0.248	0.221	0.206
R[±1, 0]	$a = 0.557$; $b = 0.742$; $\gamma = 90°$	27	0.445	0.371	0.279	0.226	0.222
R[0, ±1]	$a = 0.496$; $b = 0.785$; $\gamma = 90°$	19	0.419	0.393	0.248	0.231	0.210

intralayer structure in this case. The large difference in the intensities of the peaks at 20.05° and 22.95° is attributed to the presence of overlapping peaks due to δ- and γ-phases. The broad hump around 40° appears to be a mixture of weak broad peaks which may be attributed to (2 0) reflection of the hexagonal lattice (δ-phase) and (1 3) and (2 2) reflections of the rectangular lattice (γ-phase), as all these peaks are expected in this range. The overall dominance of the δ-phase over the γ-phase shown by both GIXR and GIXD results is supported by the singlet in the scissoring vibration band (Fig. 4(b)), as the γ-phase which is being attributed to R[1, 0] orthorhombic subcell packing, is expected to split the scissoring band. Another possible reason for the presence of a scissoring band singlet could be that the tilted alkyl chains in γ-phase do not retain their 'herringbone' character.

In the case of ZnA multilayer transferred at a subphase pH of 7.3, the reflectivity scan again clearly exhibits two types of coexisting layered structures with bilayer periods of ∼4.7 and ∼5.3 nm, which are attributed to the δ-phase and a new β-phase, the later characterized by a tilt angle of ∼19°. However, in this case, the corresponding GIXD pattern does not show any in-plane diffraction peak, indicating the absence of long range intralayer order. It is however noted from Table 2 that the tilt angle of ∼18° corresponds to another close packed structure R[0, ±1]. Although the GIXD pattern in this case does not show any features, it is interesting to note that the corresponding scissoring vibration band tends to split (Fig. 4(c)) and exhibits a main peak at 1470 cm^{-1} along with a weak shoulder at ∼1459 cm^{-1}. As explained above, the splitting is characteristic of orthorhombic subcell packing and the nature of the scissoring vibration band in this case justifies the attributing of β-phase to R[0, ±1] orthorhombic subcell packing.

The ZnA multilayer transferred at a subphase pH of 7.4 however shows a drastically different behaviour compared to the above mentioned cases. The reflectivity scan (Fig. 1(d)) exhibits the dominance of a layered structure with a bilayer period of ∼5.5 nm (α-phase) along with very weak and broad Bragg peaks corresponding to the δ-phase. The bilayer period of 5.5 nm shows that the arachidate molecules in this case are packed nearly perpendicular to the layer plane. In the corresponding GIXD pattern, out of the three low-order peaks, the peaks at 22.50° and 25.24° correspond to *d*-values of 0.40 and 0.36 nm, which nearly match with the corresponding values for (1 1) and (2 0) reflections of the R[0, 0] structure. The peak at 20.55° can again be indexed as the (1 0) reflection of the hexagonal lattice corresponding to a lattice constant of 0.5 nm, and attributed to the δ-phase, which is the weaker component in this case. Based on the above, we attribute the δ-phase to the ideal close packed herringbone structure R[0, 0] which consists of arachidate molecules packed in herringbone arrangement in a rectangular layer cell with their chain axis nearly perpendicular to the layer plane. The corresponding FT-IR spectrum shown in Fig. 3(d) strongly supports the GIXR and GIXD results as the scissoring vibration band exhibits a clear doublet characteristic of orthorhombic subcell packing with two molecules per unit cell. These results show that in the case of ZnA multilayer transferred at a subphase pH of 7.4, the dominant phase has a close packed molecular packing similar to that usually observed in LB multilayers of divalent fatty acid salts like CdA and PbA.

For the ZnA multilayers transferred at a subphase pH of 7.6, the reflectivity scan (Fig. 1(e)) is similar to that observed in the case of subphase pH of 6.8 (Fig. 1(b)). The dominant layered structure corresponds to a chain tilt angle of ∼32° along with another layered structure with a chain tilt angle of ∼25°. The GIXD pattern for this multilayer shown in Fig. 3(e) also exhibits features similar to that in Fig. 3(b), as can be seen from Table 1. Hence in this case too, the phases present are identified as δ and γ.

The dependence of the 3D structure of various phases appearing in ZnA multilayers at different subphase pH values reveals an interesting pattern. Towards the lower and higher ends of subphase pH range investigated, the 3D structure tends to acquire a relatively less dense, rotator phase like molecular packing. Between the two extremes of the subphase pH range investigated, different 3D structures corresponding to close packed arrangements based on orthorhombic subcells, but with alkyl chains tilted from the layer normal, proposed by Kitaigorodskii, appear. In a very narrow subphase pH range ∼7.4, the ideal close packed herringbone structure dominates, which has not been reported in ZnA multilayers earlier. Such dependence of 3D structure on subphase pH has not been reported in divalent fatty acid salt LB multilayers. These results on ZnA multilayers point towards the limited nature of the correlation between metal ion electronegativity and the molecular packing in multilayers of divalent fatty acid salts. The exhibition of polymorphic phases is possibly due to the complex zinc ion hydrolysis equilibria at different values of subphase pH existing in the monolayer on water surface and its effect on the structure of the transferred multilayer.

5. Conclusions

The 3D structure of ZnA multilayers has an unusually strong dependence on subphase pH, at which the monolayers are transferred. The δ-phase corresponding to the largest alkyl chain tilt angle of ∼32°, appears as a single phase around the subphase pH of 6.5 and is found to be stable over the complete pH range (6.5–8.0) investigated. The other phases, namely α, β and γ appear only in certain ranges of subphase pH. In a very narrow subphase pH range ∼7.4, the α-phase corresponding to the ideal close packed herringbone structure dominates. X ray scattering studies show that the polymorphic phases have characteristic interface morphological features, independent of the subphase pH at which the phase appears.

Acknowledgements

Financial assistance from the Department of Science and Technology, Government of India and the Indo-Italian

Programme of co-operation in Science and Technology is gratefully acknowledged. The authors also like to thank Drs. P. Dubcek, H. Amenitsch and S. Bernstorff of Sincrotrone, Trieste for their help in carrying out GIXD measurements.

References

[1] G. Roberts (Ed.), Langmuir–Blodgett Films, Plenum Press, New York, 1990.
[2] A. Ulman, Introduction to Ultrathin Organic Films, Academic Press, New York, 1991.
[3] J.K. Basu, M.K. Sanyal, Phys. Rep. 363 (2002) 1.
[4] D.K. Schwartz, Surf. Sci. Rep. 27 (1997) 41.
[5] J.A. Zasadzinski, R. Viswanathan, L. Madsen, J. Garnaes, D.K. Schwartz, Science 263 (1994) 1726.
[6] R. Stömmer, U. Englisch, U. Pietsch, V. Hòly, Physica B 221 (1996) 284.
[7] A. Malik, M.K. Durbin, A.G. Richter, K.G. Huang, P. Dutta, Phys. Rev. B 52 (1995) 11654.
[8] P. Tippmann-Krayer, R.M. Kenn, H. Möhwald, Thin Solid Films 210/211 (1992) 577.
[9] D.G. Wiesler, L.A. Feigin, C.F. Majkrzak, J.F. Ankner, T.S. Berzina, V.I. Troitsky, Thin Solid Films 266 (1995) 69.
[10] J.B. Peng, G.T. Barnes, I.R. Gentle, Adv. Colloid Interface Sci. 91 (2001) 163.
[11] A.I. Kitaigorodskii, Organic Chemical Crystallography, Consultant Bureau, New York, 1961.
[12] R. Viswanathan, L. Madsen, J.A. Zasadzinski, D.K. Schwartz, Science 269 (1995) 51.
[13] A. Dhanabalan, N. Prasanth Kumar, S. Major, S.S. Talwar, Thin Solid Films 327–329 (1998) 787.
[14] B.K. Agarwal, X-ray Spectroscopy, Springer, Berlin, 1979.
[15] A. Gibaud, N. Cowlam, G. Vignaud, T. Richardson, Phys. Rev. Lett. 74 (1995) 3205.
[16] R.E. Geer, R. Shashidhar, A.F. Thibadeaux, R.S. Duran, Phys. Rev. Lett. 71 (1993) 1391.
[17] R.G. Snyder, J. Mol. Spectrosc. 7 (1961) 116.
[18] J.F. Rabolt, F.C. Burns, N.E. Schlotter, J.D. Swalen, J. Chem. Phys. 78 (1983) 946.
[19] F. Kumura, J. Umemura, T. Takenaka, Langmuir 2 (1986) 96.
[20] N. Prasanth Kumar, S. Major, S. Vitta, S.S. Talwar, P. Dubcek, H. Amenitsch, S. Bernstorff, V. Ganesan, A. Gupta, B.A. Dasannacharya, Colloids Surf. A: Physicochem. Eng. Aspects 198–200 (2002) 75.
[21] E.B. Sirota, D.M. Singer, J. Chem. Phys 101 (1994) 10873.